Scanning the human proteome for calmodulin-binding proteins

Xinchun Shen*†‡, C. Alexander Valencia*†‡, Jack Szostak§, Biao Dong*†, and Rihe Liu*†¶

*Division of Medicinal Chemistry and Natural Products, School of Pharmacy, and †Carolina Center for Genome Sciences, University of North Carolina, Chapel Hill, NC 27599; and §Howard Hughes Medical Institute, and Department of Molecular Biology, Massachusetts General Hospital, Boston, MA 02114

Edited by Patrick O. Brown, Stanford University School of Medicine, Stanford, CA, and approved February 25, 2005 (received for review October 25, 2004)

The calcium ion (Ca^{2+}) is a ubiquitous second messenger that is crucial for the regulation of a wide variety of cellular processes. The diverse transient signals transduced by Ca^{2+} are mediated by intracellular Ca^{2+}-binding proteins, also known as Ca^{2+} sensors. A key obstacle to studying many Ca^{2+}-sensing proteins is the difficulty in identifying the numerous downstream target interactions that respond to Ca^{2+}-induced conformational changes. Among a number of Ca^{2+} sensors in the eukaryotic cell, calmodulin (CaM) is the most widespread and the best studied. Employing the mRNA display technique, we have scanned the human proteome for CaM-binding proteins and have identified and characterized a large number of both known and previously uncharacterized proteins that interact with CaM in a Ca^{2+}-dependent manner. The interactions of several identified proteins with Ca^{2+}/CaM were confirmed by using pull-down assays and coimmunoprecipitation. Many of the CaM-binding proteins identified belong to protein families such as the DEAD/H box proteins, ribosomal proteins, proteasome 26S subunits, and deubiquitinating enzymes, suggesting the possible involvement of Ca^{2+}/CaM in different signaling pathways. The selection method described herein could be used to identify the binding partners of other calcium sensors on the proteome-wide scale.

mRNA display | binding motif | protein–protein interactions | calcium-dependent

Calmodulin (CaM) is a small ubiquitously expressed EF-hand Ca^{2+}-binding protein that mediates a wide variety of cellular functions in eukaryotes (1–7). Like many other Ca^{2+}-binding proteins, Ca^{2+}-loaded CaM has a distinctly different conformation from the Ca^{2+}-free form (7). Ca^{2+}/CaM can bind to many different protein targets with high affinity (8–11). After decades of work, many Ca^{2+}/CaM-binding proteins have been identified, including Ca^{2+}/CaM-dependent protein kinases and phosphatases, proteins involved in second-messenger generation, and proteins that regulate cytoskeletal elements (12, 13). Intriguingly, protein targets of CaM continue to be discovered (10, 11, 14–16). The identification of CaM-binding targets significantly advances our understanding of many signaling transduction pathways mediated by this crucial Ca^{2+}-sensing protein.

A key obstacle to studies on Ca^{2+}-sensor proteins is the difficulty in identifying their downstream targets because of the technical limitations of various methods that have been used, especially on a proteome-wide scale. Phage display has been used to isolate CaM-binding sequences from short synthetic peptide libraries, but the selected CaM-binding sequences were poorly correlated with naturally occurring proteins (17). Yeast two-hybrid analysis is another method that is widely used to study protein–protein interactions. Recently, the yeast two-hybrid system has been used in a high throughput mode to construct comprehensive protein–protein interaction maps for several organisms, including the unicellular yeast *Saccharomyces cerevisiae* (18) and the multicellular organisms *Drosophila melanogaster* (19) and the nematode *Caenorhabditis elegans* (20). However, in each of the genome-wide protein–protein interaction maps, only a limited number of CaM-binding proteins were reported, and most of the known CaM-binding proteins are missing. Proteome chips have also been used as a high throughput approach to identifying protein–protein interactions. Indeed, a yeast proteome chip has been used to identify CaM-binding proteins (21). However, the preparation of a proteome chip from any multicellular organism is a major undertaking. So far, the conventional SDS/PAGE gel overlay with recombinant, radiolabeled CaM is still the most commonly used method for the identification and characterization of CaM-binding proteins, although it is time-consuming and the number of CaM-binding proteins it can reveal is limited (11, 15). Therefore, new methodologies are necessary to identify the downstream binding partners of CaM. mRNA display is a relatively new technology that circumvents a number of difficulties associated with yeast two-hybrid and phage display (22–24). Because of the covalent linkage between the genotype and the phenotype, mRNA display provides a powerful means for reading and amplifying a protein sequence after it has been selected from large libraries (10^{12} to 10^{13} different sequences).

In this article, we describe the use of this amplification-based *in vitro* protein selection technique to identify a large number of known and previously uncharacterized Ca^{2+}/CaM-binding proteins from the human proteome.

Materials and Methods

Construction of cDNA Library and Generation of an mRNA-Displayed Proteome Library. Poly(A)$^+$ mRNAs from different human tissues, including the brain, heart, spleen, thymus, and muscle (Stratagene) were mixed as a pool. A cDNA library was constructed as detailed in *Supporting Materials and Methods*, which is published as supporting information on the PNAS web site. The mRNA-displayed proteome library was generated as described in refs. 23 and 25. The resulting mRNA-displayed proteome library was then successively purified on the basis of the E and FLAG affinity tags at the N and C termini, respectively.

Selection of Ca^{2+}-Dependent CaM-Binding Proteins from mRNA-Displayed Human Proteome Library. The general selection scheme is given in Fig. 1. The purified mRNA-displayed proteome library (≈1.5 pmol each round) was first diluted in the selection buffer (50 mM Tris·HCl, pH 7.5/150 mM KCl/0.05% Tween 20/1 mg/ml BSA/5 mM 2-mercaptoethanol/0.5 mM Ca^{2+}) and passed through a precolumn of 100 μl of streptavidin beads (Pierce). The flowthrough was incubated with 25 μg of biotinylated CaM (*Supporting Materials and Methods*) for 1 h at 4°C. After binding, the mixture was incubated with 100 μl of pre-

This paper was submitted directly (Track II) to the PNAS office.

Abbreviation: CaM, calmodulin.

‡X.S. and C.A.V. contributed equally to the work.

¶To whom correspondence should be addressed. E-mail: rliu@email.unc.edu.

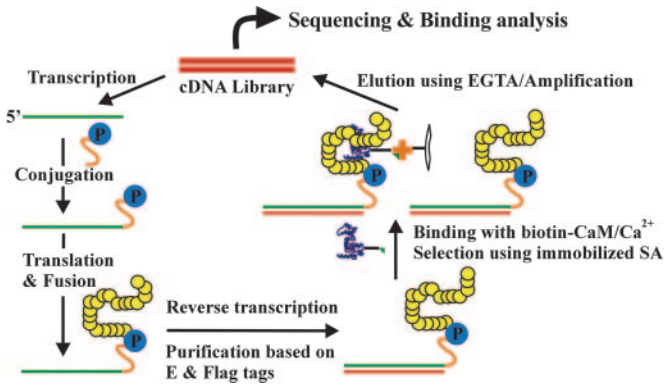

Fig. 1. Selection of CaM-binding proteins by using an mRNA-displayed human proteome library. mRNA, green; DNA, red; protein, yellow; puromycin, blue circle. SA, streptavidin beads.

washed streptavidin beads for another 30 min, followed by loading into an empty column. Unbound and nonspecifically bound molecules were washed off the column by using 18 column volumes of selection buffer. Molecules that bound to CaM in a Ca^{2+}-dependent manner were eluted by using the same buffer containing 2 mM EGTA. The selected molecules were PCR-amplified for the next round of selection or cloned into a TOPO vector (Invitrogen) for sequencing and analysis.

***In Vitro* CaM-Binding Assay and Affinity Measurement.** Individually cloned sequences selected from round 1 or round 2 were PCR-amplified and used as a template for a coupled *in vitro* transcription/translation reaction in the presence of 10 μCi (1 Ci = 37 GBq) [^{35}S]methionine (PerkinElmer) in a total volume of 25 μl for 90 min at 30°C. The expressed protein fragment or full-length protein was purified by using a Ni^{2+}-nitrilotriacetic acid (NTA) (Qiagen, Valencia, CA) or Co^{2+}-NTA (Clontech) column. Selected fragments were used for the measurement of binding affinity as follows. An aliquot of purified protein fragment was mixed with an appropriate amount of biotinylated CaM (from 1 nM to 2.5 μM final concentration) in CaM-binding buffer A (25 mM Tris·HCl, pH 8.0/150 mM NaCl/1 mg/ml BSA/5 mM 2-mercaptoethanol/1 mM $CaCl_2$) for 90 min at 4°C. After binding, 30 μl of a 50% slurry of streptavidin beads was added, and the mixture was incubated for 45 min at room temperature with gentle mixing. The supernatant was removed by centrifugation in an Ultrafree-MC centrifugal filter tube (Millipore). The beads were washed three times with 150 μl of buffer A. Proteins captured were then released from the column by chelating Ca^{2+} with 150 μl of elution buffer containing 2 mM EGTA. The extent of binding was determined by scintillation counting each fraction, including the recovered beads. To determine the binding affinity, the data were fit to a binding curve by using the SIGMAPLOT (Systat, Point Richmond, CA) software.

Cell Culture and Mouse Brain Lysate Preparation. HeLa S3 cells were grown to stationary phase in Ham's F12 medium supplemented with 10% FBS. Cells were harvested and lysed as described in ref. 26. To prepare mouse brain lysates, the brains of 8- to 10-month-old mice were homogenized in cold lysis buffer immediately after decapitation. After centrifugation to remove intact cells, the supernatants were cleared at 21,000 $\times$ *g* for 15 min at 4°C. The lysates that were prepared were used for pull-down assays or coimmunoprecipitation.

CaM-Sepharose Pull-Down Assay. Approximately 100 μl of pre-equilibrated CaM-Sepharose 4B beads (Amersham Pharmacia) were added to the lysate ($\approx$1 mg of total protein), followed by incubation for 4 h at 4°C in a buffer containing 50 mM Tris·HCl (pH 7.4), 150 mM NaCl, EDTA-free protease inhibitors (Roche, Indianapolis), and either 1 mM $CaCl_2$ (buffer B) or 2 mM EGTA (buffer C). The beads were washed five times with buffer B or buffer C. Proteins that bound to CaM in a Ca^{2+}-dependent manner were eluted from the beads with buffer C containing 2 mM EGTA. Proteins from each fraction were resolved on SDS/PAGE gels, transferred to a nitrocellulose membrane (Amersham Pharmacia), and probed with an antibody against the protein of interest.

Coimmunoprecipitation. Equal amounts of precleared whole-cell lysate ($\approx$1 mg of total protein) were incubated with 2 μg of primary antibody (anti-CaM, Santa Cruz Biotechnology) for 4 h at 4°C in the presence of buffer B or buffer C. Approximately 20 μl of preequilibrated protein A/G-agarose conjugate was added, and the mixture was further incubated for 2 h at 4°C with mixing. The pellet was collected and washed three times with buffer B or buffer C. After the final wash, Ca^{2+}/CaM-binding proteins were eluted from pellets by using buffer C containing 2 mM EGTA. Different fractions were loaded onto SDS/PAGE, followed by Western blotting and probing.

Supporting Information. For further information, see *Supporting Sequence Information*, Figs. 5–16, and Table 3, which are published as supporting information on the PNAS web site.

Results and Discussion

Because random priming was used to initiate first-strand cDNA synthesis, most sequences in the initial library were out-of-frame or contained sequences from 5′- or 3′-UTRs. To generate a high quality protein library for CaM-binding selection, one round of preselection by using mRNA display was performed (27) by successive purification of mRNA-displayed proteins based on affinity tags at the N and C termini. Because only in-frame transcripts display the C-terminal affinity tag and internally initiated transcripts lack the N-terminal tag, sequences with continuous ORFs were enriched and sequences that contained frameshifts or untranslated regions were removed during the preselection process (data not shown). Because the initial library contained $\approx 10^{12}$ protein molecules (1.5 pmol), every expressed gene should be represented by numerous copies of distinct gene fragments. The possibility of identifying proteins encoded by rare genes is, therefore, significantly increased. Fig. 1 shows the general scheme for selecting CaM-binding proteins from the mRNA-displayed human proteome library. Biotinylated CaM from bovine brain (*Supporting Materials and Methods*), which is identical to human CaM in amino acid sequences, was used as the target for selection. The formation of Ca^{2+}/CaM/binding partner complexes was performed in a homogenous solution, and the complexes were captured by streptavidin-agarose beads. Unbound members of the library were washed away, whereas molecules that bound to CaM in a Ca^{2+}-dependent manner were specifically eluted by using an elution buffer containing EGTA. The enriched library was then regenerated by PCR, *in vitro* transcription, crosslinking, *in vitro* translation and fusion, reverse transcription, and affinity purifications before it was used for the subsequent round of selection (23, 28). Approximately 0.25% of the input of radiolabeled, mRNA-displayed protein molecules was specifically eluted from the streptavidin agarose beads in round 1 by chelating Ca^{2+} with EGTA, and this result increased to $\approx$8.5% in round 2 (Fig. 5).

We first analyzed the selected molecules from round 2 by cloning and sequencing, followed by BLAST searches to identify the proteins present in this pool. Among the 77 sequences we analyzed in round 2, there were 28 distinct sequence clusters, among which 21 were from known proteins and 7 from hypo-

Table 1. Potential previously uncharacterized Ca^{2+}/CaM-binding proteins isolated from the first round of selection

Protein	Accession no.	ID no.
CASP8-associated protein 2	AAH56685	1
F-box only protein 9	NP_258442	2
Smcx homolog	NP_004178	3
Transmembrane protein 10	AAH33737	4
Splicing factor, R/S-rich 5	AAH18823	5
Dystonin	NP_056363	6
Optineurin	AAH32762	7
Ribosomal protein S8	NP_001003	8
Ribosomal protein S4	AAH10286	9
CDC 37-like 1	AAH14133	10
GNAS complex locus	NP_000507	11
Programmed cell death 7	NP_005698	12
Leucine zipper protein	AAL78672	13
Radixin	AAH02626	14
General transcription factor II-i	NP_127494	15
Ubiquitin C-terminal hydrolase UCH37 or UCHL5	NP_057068	16
RAD23 homolog B	NP_002865	17
CDC5-like	AAH01568	18
Kinesin family member 1B	NP_055889	19
Syntaxin 8	AAP35983	20
Dimethylarginine dimethylaminohydrolase 1	AAH33680	21
A kinase (PRKA) anchor protein 6	NP_004265	22
Peptidylglycine α-amidating monooxygenase	AAP36087	23
SRP 14 kDa	AAH71716	24
Zinc finger protein 291	NP_065894	25
Dedicator of cytokinesis 3	AAP80572	26
HECT domain and RLD2	NP_004658	27
eIF3, subunit 8	NP_003743	28
Splicing factor 3b, subunit 1	AAH56155	29
Fat-3	XP_061864	30
Synaptopodin 2	XP_050219	31
v-Myb myeloblastosis viral oncogene homolog	XP_034274	32
TBC1 domain family, 4	XP_375032	33
Stromal antigen 1	NP_005853	34
26S subunit, non-ATPase, 12	NP_002807	35
DnaJ homolog, subfamily C	NP_056083	36
Predicted KIAA1345 protein	XP_106386	37
Matrin 3	NP_061322	38
XRCC4	AAH05259	39
FK506 binding protein 3	AAP35550	40
Nesprin 2	NP_055995	41
Sorting nexin 6	AAH01798	42
Translationally controlled tumor protein, 1	AAH52333	43
Armadillo repeat containing protein	NP_060590	44
DEAD box polypeptide 21	NP_004719	45
RAN binding protein 2	NP_006258	46
Membrane component, surface marker 2	NP_114068	47
Nexilin (F actin binding protein)	NP_653174	48
Transcription factor MRG15-2	AAN65338	49

Table 1. (continued)

Protein	Accession no.	ID no.
5′-Purine nucleotidase, II	AAH01595	50
LIM domain only 7	NP_005349	51
Chromosome 10 ORF 6	NP_060591	52
Lymphocyte antigen 96	AAH20690	53
SNRP polypeptide B	NP_003083	54
MBIP	NP_057670	55
MYC binding protein C	NP_996557	56
RNA polymerase, polypeptide B	AAH23503	57
Creatine kinase, mitochondrial 1	NP_066270	58
ATRX isoform 1	NP_000480	59
Peptidylprolyl isomerase-like 2	AAH28385	60
Acyl-coenzyme A dehydrogenase medium chain	AAH05377	61
v-AKT 1	NP_005154	62
LUC7-like isoform β	NP_958815	63
HECT domain protein LASU1	BAC06833	64
Nebulin	NP_004534	65
DEAH box polypeptide 57	NP_663621	66
Hypothetical protein FLJ13213	AAH46119	67
Integrin alpha chain, α 6	NP_000201	68
Lactamase-β, mitochondrial	NP_116246	69
Nuclease-sensitive element-binding protein 1	NP_004550	70
Dedicator of cytokinesis 11	AAH47713	71
Hypothetical protein FLJ12892	NP_073594	72
DEAD box polypeptide 5	AAP35589	73
S100B	NP_006263	74
Ribosomal protein S15a	AAH46113	75
26S subunit, non-ATPase, 2	AAH07897	76
Triadin	CAD33526	77
SET translocation	AAH32749	78
Restin isoform b	NP_937883	79
Ubiquitin specific protease-M or USP16	AAH30777	80
Ribosomal protein L22	NP_000974	81
Ribosomal protein S14	AAH06784	82
Stromal interaction molecule 2	NP_065911	83
Peroxiredoxin 1	NP_859048	84
Heart motor protein	BAA04656	85
XTP5	AAO85462	86
Nucleolar protein 7, 27 kDa	AAH62683	87
Predicted KIAA0522 protein	XP_291345	88
Phosphatase and actin regulator 4	NP_076412	89
Enthoprotin	DAA00062	90
MYC binding protein 2	NP_055872	91
Zinc finger protein 450	NP_055612	92
Dmx-like 1	NP_005500	93
Ribosomal protein L13a	NP_036555	94
Sequestosome 1	AAH19111	95
WD repeat domain 9 isoform B	NP_387505	96
Methionyl aminopeptidase 2	NP_006829	97
Hypothetical protein FLJ30655	BAB70876	98

thetical or unknown proteins. The pool was dominated by a few known CaM-binding proteins. Of 77 sequences, 48 were from 6 classes of well known CaM-binding proteins, including different isoforms (α, β, γ, and δ) of Ca^{2+}/CaM-dependent protein kinases (20 clones), different isoforms (α, β, and γ) of Ca^{2+}/CaM-dependent protein phosphatases (9 clones), Ca^{2+}-transporting ATPase (11 clones), α II spectrin (4 clones), phosphoinositide-3-kinase (3 clones), and myosin heavy polypeptide 1 (1 clone). All of these sequences contained a known or putative CaM-binding motif (Figs. 7–16), indicating that their enrichment was indeed due to their binding to Ca^{2+}/CaM.

Because the pool from round 2 was dominated by a small number of well known CaM-binding proteins, we focused our effort on analyzing the sequences enriched from the first round of selection. The sequences selected in round 1 were diverse and not dominated by any particular proteins. Among 499 clones we analyzed in round 1, 110 sequences were from 28 known CaM-binding proteins (Table 3). A number of these proteins were identified as multiple copies. From the remaining 389

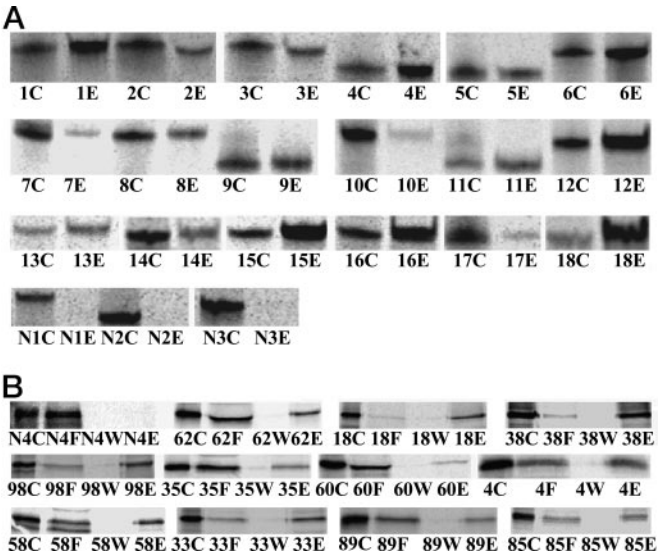

Fig. 2. *In vitro* binding analysis of selected proteins with biotin-CaM. Full-length proteins or fragments were generated by a transcription/translation (TNT) reaction. An aliquot of the TNT mixture was incubated with an appropriate amount of biotinylated CaM in the presence of 1 mM $CaCl_2$, followed by mixing with streptavidin-agarose beads. The beads were washed, and the bound molecules were eluted by using a buffer containing 2 mM EGTA. (*A*) Selected protein fragments, showing expressed protein (C) and eluent (E). The complete fragment binding data corresponding to proteins listed in Table 1 are provided in Fig. 6. The last three samples (N1-N3) are negative controls. N1 (similar to cardiac morphogenesis protein) and N2 (MLL3 protein) are two protein fragments that do not bind to CaM in the binding assays. N3 is a protein fragment from the non-CaM binding region of a known CaM-binding protein (ATP2B1). (*B*) Full-length proteins, showing expressed protein (C), the flowthrough (F), the last wash (W), and the eluent (E). N4, negative control (KIAA0367 from an irrelevant project). The names of all other proteins are listed in Table 1 according to their IDs.

sequences, we were able to identify 269 annotated or hypothetical unique proteins. We tested whether these selected protein fragments bound to CaM by using the *in vitro* CaM-binding assay described above. A number of positive and negative controls were tested, and the results confirmed that this method is suitable for studying the binding between Ca^{2+}/CaM and proteins of interest (data not shown). Using this binding assay, we found that almost all of the annotated proteins identified in round 2 bound to CaM in a Ca^{2+}-dependent manner. Among the 269 annotated or hypothetical unique proteins from round 1, we identified 98 previously uncharacterized CaM-binding protein fragments (Table 1 and Figs. 2*A* and 6). Therefore, ≈42% of unique proteins identified in round 1 were known or potential previously uncharacterized CaM-binding proteins. Of the selected proteins that bound to CaM, the interactions were indeed Ca^{2+}-dependent. To test whether the full-length proteins also bind to CaM as expected, we expressed several proteins of interest by coupled *in vitro* transcription and translation and studied their binding to Ca^{2+}/CaM by using the same *in vitro* assay. Fig. 2*B* shows that these full-length proteins also bound to CaM in a Ca^{2+}-dependent manner.

The Ca^{2+}/CaM-binding motifs present in target proteins are quite diverse and have been grouped into three related classes, namely the 1-14 motif, the 1-10 motif, and the 1-16 motif, in addition to the Ca^{2+}-independent IQ motif (13, 29). Each group contains several subclasses. A robust selection strategy should allow the identification of proteins containing all of these different classes of CaM-binding motifs. Sequence analysis of known CaM-binding proteins isolated in our selection demonstrates that all classes and almost all known subclasses of

Table 2. Binding affinity of some selected previously uncharacterized CaM-binding protein fragments with Ca^{2+}/CaM

Protein	Accession no.	K_d, nM
26S subunit, non-ATPase, 2	AAH07897	11 ± 3
26S subunit, non-ATPase, 12	NP_002807	214 ± 40
Armadillo repeat-containing protein	NP_060590	382 ± 53
ATRX	NP_000480	1248 ± 250
CDC5-like	AAH01568	15 ± 2
Dmx-like 1	NP_005500	59 ± 7
Enthoprotin	DAA00062	85 ± 16
GTFII-i	NP_127494	131 ± 30
LIM domain only 7	NP_005349	19 ± 13
M phase phosphoprotein 8	AAH03542	36 ± 14
Peptidylglycine α-amidating monooxygenase	AAP36087	9 ± 4
Programmed cell death 7	NP_005698	200 ± 27
RAD23B	NP_002865	20 ± 3
Radixin	AAH02626	70 ± 13
Ribsome protein S15a	AAH46113	239 ± 120
SRP 14 kDa	AAH71716	331 ± 156
Sorting nexin 6	AAH01798	528 ± 74
Splicing factor 3b, subunit 1	AAH56155	703 ± 375
Splicing factor, R/S-rich 5	AAH18823	893 ± 646
Synaptopodin 2	XP_050219	147 ± 52
TBC1 domain family, 4	XP_375032	9 ± 2
Transmembrane protein 10	AAH33737	48 ± 5
Ubiquitin C-terminal hydrolase UCH37 or UCHL5	NP_057068	453 ± 211
Zinc finger protein 291	NP_065894	1005 ± 153

CaM-binding motifs were identified by using this strategy. They include the 1-5-8-14 subclass (titin, plasma membrane calcium pump, and calcineurin A), the basic 1-8-14 subclass (CaM-dependent protein kinase IV and smooth muscle myosin light chain kinase), the 1-8-14 subclass (α-fodrin), the 1-14 subclass (CaMK I), the 1-5-10 subclass (HSP90, phosphatidylinositol 3-kinase), the basic 1-5-10 subclass (CaMK II), the 1-16 class (CaMKK-α), and the IQ or IQ-like class (dynein, myosin, skeletal muscle myosin heavy polypeptide 2, and type III sodium channel protein). These results demonstrate that our method allows efficient identification of Ca^{2+}/CaM-binding proteins with various binding motifs from the human proteome.

The ease of mapping the binding motifs is one advantage of our method. The CaM-binding motif of a selected protein can be readily mapped by locating the shortest overlapping region from different selected fragments of the parental protein. Among 499 clones analyzed from round 1, 14 were from α-fodrin, a well-characterized CaM-binding protein. These 14 protein fragments ranged from 80 to 189 residues and overlapped from M1158-N1192 (MMPRDETDSKT*ASPWKSARLMVHTVAT-FNSI*KELN) (Fig. 7). This 34 amino acid fragment is just 14 amino acids longer than the previously mapped CaM-binding motif of α-fodrin (A1169-I1188, italicized) (13). Similar results were obtained from many other well characterized CaM-binding proteins (Figs. 8–11). The CaM-binding motifs in the previously uncharacterized CaM-binding proteins were generally predicted to contain a positively charged amphiphilic α-helix when the selected sequence fragments were analyzed by using a Web-based motif analysis program (13).

We determined the binding affinities of a number of selected CaM-binding proteins by varying the concentration of biotinylated CaM used in the binding assay (Table 2). The binding affinities we obtained for the known CaM-binding proteins calcineurin and myosin light-chain kinase were similar to those reported in refs. 30 and 31). We found that the binding affinities

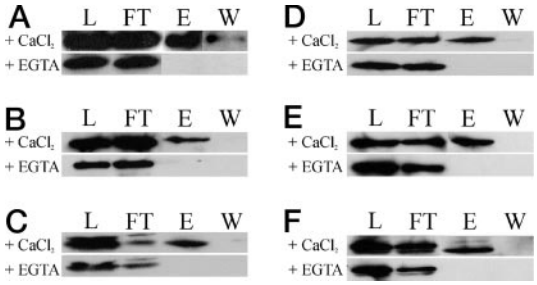

Fig. 3. Calcium-dependent interactions between calmodulin and AKT1, CDC5-L, and RAD23B. CaM-Sepharose pull-down assays by using mouse brain lysate (*A–C*) and human HeLa cell lysate (*D–F*). Lysates were incubated with CaM-Sepharose 4B beads in the presence of $CaCl_2$ (*Upper*) or EGTA (*Lower*) as described in the experimental section. L, lysate; FT, flowthrough; E, elution; W, wash. (*A* and *D*) AKT-1. (*B* and *E*) CDC5-L. (*C* and *F*) RAD23B. Anti-AKT1 and anti-CaM were from Santa Cruz Biotechnology, anti-CDC5L from BD Biosciences, and anti-RAD23B from Rockland (Gilbertsville, PA).

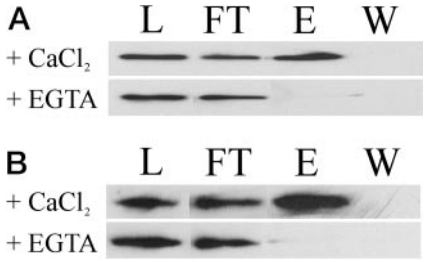

Fig. 4. Coimmunoprecipitation from HeLa cell lysate of AKT-1 and CDC5-L with CaM. Equal amounts of precleared HeLa cell lysate were incubated with anti-CaM antibody in the presence of CaM-binding buffer containing either 1 mM $CaCl_2$ or 2 mM EGTA. The protein complex was captured by protein A/G-agarose conjugate and eluted with buffer C. AKT or CDC5L associated with CaM was detected by Western blot analysis by using anti-AKT (*A*) or anti-CDC5L (*B*). L, lysate; FT, flowthrough; E, elution of pellets by using buffer C; W, wash of pellets by using buffer B.

of our previously uncharacterized CaM binding proteins ranged from 5 nM to 2 μM, suggesting that CaM-binding proteins with a wide range of binding affinities could be identified. Interestingly, we found that a number of proteins bound to Ca^{2+}/CaM with affinities >300 nM. A recent study has provided evidence that interactions with Ca^{2+}/CaM with binding affinities close to 1 μM could still be physiologically significant (16).

Interactions between several previously uncharacterized CaM-binding proteins and CaM were further demonstrated by CaM-Sepharose pull-down assays. Fig. 3 shows that AKT-1, CDC5-L, and RAD23B were detected in CaM-Sepharose-bound proteins in a Ca^{2+}-dependent fashion in both mouse brain and human HeLa cell lysates. When EGTA was present in the binding buffer, the binding of these proteins to CaM-Sepharose was totally abolished. We next investigated whether endogenous CaM and two proteins of interest, AKT-1, and CDC5-L, interact *in vivo* by coimmunoprecipitation assays. As shown in Fig. 4, AKT-1 and CDC5-L were coimmunoprecipitated with Ca^{2+}/CaM, indicating that the AKT-1/Ca^{2+}/CaM and CDC5-L/Ca^{2+}/CaM complexes are indeed present *in vivo*. Because direct binding of full-length AKT-1 and CDC5L with CaM has been demonstrated *in vitro* (Fig. 2*B*), the observed interactions with CaM were presumably direct rather than mediated by other proteins.

Recent studies imply that Ca^{2+}/CaM might be a regulator of AKT activation (32), but it remained unclear as to whether the interaction of AKT with Ca^{2+}/CaM is direct or is mediated by an auxiliary protein. Our results provide strong evidence that Ca^{2+}/CaM is a direct regulator of AKT *in vivo*. Rad23A (hHR23A) and Rad23B (hHR23B) are two human homologs of the *S. cerevisiae* RAD23, which are involved in both nucleotide excision repair and ubiquitin-mediated proteolysis (33–38). Rad23 proteins contain UbL and UBA domains that can interact with the proteasome and multiubiquitin chains, respectively. Recently, it was found that Rad23 could act as a multiubiquitin chain receptor and is involved in translocating proteolytic substrates to the proteasome and promoting their degradation. The identification of Rad23B as a Ca^{2+}/CaM-binding protein prompted us to speculate that Rad23A might have a similar function. Indeed, Rad23A bound to CaM in a pull-down assay (data not shown). These results suggest that Ca^{2+}/CaM might play an important role in regulating the multiubiquitin chain recognition mediated by Rad23.

A number of the CaM-binding proteins identified in this work belong to protein families such as the DEAD/H box proteins, ribosomal proteins, zinc finger proteins, heat shock proteins, proteasome 26S subunits, and deubiquitinating enzymes. These proteins are involved in diverse pathways, including RNA unwinding and ubiquitin-mediated protein degradation. DEAD/H box proteins belong to a rapidly growing family of RNA helicases, which have been implicated in a number of cellular processes (39, 40). One of the essential questions that remains to be answered is how the DEAD/H-box proteins are regulated at the correct place and time. Three DEAD/H box proteins, namely DDX5, DDX21, and DDX57, were identified as Ca^{2+}/CaM-binding proteins from our selection, suggesting a possible link between Ca^{2+} signaling and RNA unwinding. Indeed, it has been reported that DDX5 (p68 RNA helicase) bound to CaM in a Ca^{2+}-dependent fashion and that this interaction inhibited p68 ATPase activity (41). We found that the CaM-binding motif involved in this regulation is most likely a Ca^{2+}-dependent positively charged amphiphilic α-helix (^{227}RLIDFLECGKTNLRR) (Fig. 15), rather than a Ca^{2+}-independent IQ-containing sequence (^{554}IQTSFR) as hypothesized in ref. 41. Furthermore, similar Ca^{2+}/CaM-binding motifs were also present in the selected fragments of the other two DEAD/H proteins, which indicates that the RNA unwinding activity of these DEAD/H proteins may also be regulated by their Ca^{2+}/CaM-binding motifs.

In addition to Rad23 proteins, several other proteins that are involved in the ubiquitin-proteasome pathway were also identified as Ca^{2+}/CaM-binding proteins, namely proteasome 26S subunits (PSMD2 and PSMD12) and deubiquitinating enzymes (UCHL5 and UBP-M). These results imply a possible role for CaM in this important pathway. It has been reported that purified 26S proteasomes could degrade aged Ca^{2+}/CaM and native Ca^{2+}-free CaM without ubiquitination (42). One possible explanation is that Ca^{2+}-free or Ca^{2+}-loaded CaM binds to some components of the 26S proteasome and such binding allows its entry into the proteasome without ubiquitination. It was hypothesized that such components are most likely located on the ATPase subunits of the 19S regulatory particle (42). Our finding that Ca^{2+}/CaM binds to PSMD2 and PSMD12 implies that the recognition of CaM by the 26S proteasome is mediated by non-ATPase rather than by ATPase subunits of the 19S particle. This result is consistent with the yeast proteome chip data showing that the RPN11 subunit (the human homolog is PSMD14) of the 19S regulatory particle is a CaM-binding protein (21). The finding that at least two deubiquitinating enzymes are Ca^{2+}/CaM-binding proteins is intriguing. It has been reported that UCH37 is the major deubiquitinating enzyme associated with the 26S proteasome in fission yeast (43). UBP-M has been found to be phosphorylated at the onset of mitosis and dephosphorylated during the metaphase/anaphase transition (44) in mammalian cells. It is hypothesized that UBP-M may play an important role in regulating mitotic chromatin by selectively deubiquitinating one or more critical proteins that are involved in the condensation of mitotic chromosomes. Our finding suggests that Ca^{2+}/CaM could

be involved in regulating the ubiquitin chain degradation by deubiquitinating enzymes. In addition, it has been reported that CaM is reversibly monoubiquitinated by a ubiquitin-calmodulin ligase in the presence of Ca^{2+}, and that monoubiquitination strongly decreases the biological activity of CaM toward phosphorylase kinase by reducing its affinity and the maximal degree of activation (45). An important question is how the monoubiquitination of CaM is regulated. Our result suggests that CaM deubiquitination could be catalyzed by deubiquitinating enzymes and that the regulation of CaM function by monoubiquitination could be biologically significant.

Some ribosomal proteins have been shown to interact with CaM (46, 47). We have identified six human ribosomal proteins that interact with Ca^{2+}/CaM, including 40S ribosomal proteins RPS4, RPS8, RPS14, RPS15a, and 60S ribosomal proteins RPL13a and RPL22. These results provide the basis for further investigation of how the binding of ribosomal proteins to Ca^{2+}/CaM modulates ribosome assembly and/or the process of translation.

Based on three published genome-wide protein–protein interaction maps, it appears that the yeast two-hybrid approach is not well suited for identifying Ca^{2+}-dependent protein–protein interactions (18–20), presumably because Ca^{2+} levels are tightly regulated in yeast (48, 49). Recently, a yeast proteome chip was used to study interactions of yeast proteins with CaM from bovine brain (21). From this study, 39 known or potentially uncharacterized CaM-binding proteins were identified in the yeast proteome. Although the proteome chip approach allows high throughput studies on protein–protein interactions, preparation of a proteome chip from any multicellular organism is very time-consuming and challenging. The mRNA-display approach described herein has the great advantage of using cellular mRNAs from any organism. Our results demonstrate that mRNA display can be used to efficiently map protein–protein interactions on a proteome-wide scale and may be especially useful for conditional interactions, such as interactions that are dependent on the cellular Ca^{2+} concentrations. Although mRNA display is a powerful method that allows for efficient enrichment of protein targets by iterative rounds of selection based on their interaction with a ligand of interest, this method also has its limitations. The efficiency with which a specific sequence is selected depends on a number of factors, including its abundance in the initial mRNA library, the overall efficiency of amplification, the efficiency of protein expression and mRNA fusion, and its affinity to CaM. Because of these biases, some CaM-binding proteins may not be identified. In addition, protein fragments rather than full-length proteins are selected. Thus, other approaches should be used to confirm that the identified interactions occur under physiological conditions. Nevertheless, the use of the mRNA-display approach has contributed to the comprehensive cataloging of Ca^{2+}/CaM-binding proteins. The selection methodology described herein could be applied to the high throughput identification of binding partners of different calcium sensors on a proteome-wide scale. Furthermore, this method facilitates the mapping of the binding motifs and interaction sites, which are important in understanding protein–protein interaction networks.

We thank Dr. Xiangdong Lu for assistance in providing the mouse organs and Steve Cotten for designing the artwork. This work was supported by startup funds from the Carolina Center for Genome Sciences and School of Pharmacy at University of North Carolina at Chapel Hill (to R.L.), Damon Runyon-Walter Winchell Foundation Cancer Research Fund Grant DRG1430 (to R.L.), and National Institutes of Health Grant GM53936 (to J.S.). J.S. is an investigator of the Howard Hughes Medical Institute.

1. Ghosh, A. & Greenberg, M. E. (1995) *Science* **268,** 239–247.
2. Clapham, D. E. (1995) *Cell* **80,** 259–268.
3. Bootman, M. D. & Berridge, M. J. (1995) *Cell* **83,** 675–678.
4. Berridge, M. J., Bootman, M. D. & Roderick, H. L. (2003) *Nat. Rev. Mol. Cell Biol.* **4,** 517–529.
5. Carafoli, E., Santella, L., Branca, D. & Brini, M. (2001) *Crit. Rev. Biochem. Mol. Biol.* **36,** 107–260.
6. Orrenius, S., Zhivotovsky, B. & Nicotera, P. (2003) *Nat. Rev. Mol. Cell Biol.* **4,** 552–565.
7. Ikura, M. (1996) *Trends Biochem. Sci.* **21,** 14–17.
8. James, P., Vorherr, T. & Carafoli, E. (1995) *Trends Biochem. Sci.* **20,** 38–42.
9. O'Neil, K. T. & DeGrado, W. F. (1990) *Trends Biochem. Sci.* **15,** 59–64.
10. Chin, D. & Means, A. R. (2000) *Trends Cell Biol.* **10,** 322–328.
11. O'Day, D. H. (2003) *Cell Signalling* **15,** 347–354.
12. Crivici, A. & Ikura, M. (1995) *Annu. Rev. Biophys. Biomol. Struct.* **24,** 85–116.
13. Yap, K. L., Kim, J., Truong, K., Sherman, M., Yuan, T. & Ikura, M. (2000) *J. Struct. Funct. Genomics* **1,** 8–14.
14. Junge, H. J., Rhee, J. S., Jahn, O., Varoqueaux, F., Spiess, J., Waxham, M. N., Rosenmund, C. & Brose, N. (2004) *Cell* **118,** 389–401.
15. Reddy, V. S., Ali, G. S. & Reddy, A. S. (2002) *J. Biol. Chem.* **277,** 9840–9852.
16. Rakhilin, S. V., Olson, P. A., Nishi, A., Starkova, N. N., Fienberg, A. A., Nairn, A. C., Surmeier, D. J. & Greengard, P. (2004) *Science* **306,** 698–701.
17. Dedman, J. R., Kaetzel, M. A., Chan, H. C., Nelson, D. J. & Jamieson, G. A., Jr. (1993) *J. Biol. Chem.* **268,** 23025–23030.
18. Uetz, P., Giot, L., Cagney, G., Mansfield, T. A., Judson, R. S., Knight, J. R., Lockshon, D., Narayan, V., Srinivasan, M., Pochart, P., *et al.* (2000) *Nature* **403,** 623–627.
19. Giot, L., Bader, J. S., Brouwer, C., Chaudhuri, A., Kuang, B., Li, Y., Hao, Y. L., Ooi, C. E., Godwin, B., Vitols, E., *et al.* (2003) *Science* **302,** 1727–1736.
20. Li, S., Armstrong, C. M., Bertin, N., Ge, H., Milstein, S., Boxem, M., Vidalain, P. O., Han, J. D., Chesneau, A., Hao, T., Goldberg, D. S., *et al.* (2004) *Science* **303,** 540–543.
21. Zhu, H., Bilgin, M., Bangham, R., Hall, D., Casamayor, A., Bertone, P., Lan, N., Jansen, R., Bidlingmaier, S., Houfek, T., *et al.* (2001) *Science* **293,** 2101–2105.
22. Roberts, R. W. & Szostak, J. W. (1997) *Proc. Natl. Acad. Sci. USA* **94,** 12297–12302.
23. Liu, R., Barrick, J. E., Szostak, J. W. & Roberts, R. W. (2000) *Methods Enzymol.* **318,** 268–293.
24. Takahashi, T. T., Austin, R. J. & Roberts, R. W. (2003) *Trends Biochem. Sci.* **28,** 159–165.
25. Kurz, M., Gu, K. & Lohse, P. A. (2000) *Nucleic Acids Res.* **28,** E83.
26. McCullar, J. S., Larsen, S. A., Millimaki, R. A. & Filtz, T. M. (2003) *J. Biol. Chem.* **278,** 33708–33713.
27. Cho, G., Keefe, A. D., Liu, R., Wilson, D. S. & Szostak, J. W. (2000) *J. Mol. Biol.* **297,** 309–319.
28. Hammond, P. W., Alpin, J., Rise, C. E., Wright, M. & Kreider, B. L. (2001) *J. Biol. Chem.* **276,** 20898–20906.
29. Rhoads, A. R. & Friedberg, F. (1997) *FASEB J.* **11,** 331–340.
30. Hubbard, M. J. & Klee, C. B. (1987) *J. Biol. Chem.* **262,** 15062–15070.
31. Lukas, T. J., Burgess, W. H., Prendergast, F. G., Lau, W. & Watterson, D. M. (1986) *Biochemistry* **25,** 1458–1464.
32. Deb, T. B., Coticchia, C. M. & Dickson, R. B. (2004) *J. Biol. Chem.* **279,** 38903–38911.
33. Schauber, C., Chen, L., Tongaonkar, P., Vega, I., Lambertson, D., Potts, W. & Madura, K. (1998) *Nature* **391,** 715–718.
34. Chen, L. & Madura, K. (2002) *Mol. Cell. Biol.* **22,** 4902–4913.
35. Verma, R., Oania, R., Graumann, J. & Deshaies, R. J. (2004) *Cell* **118,** 99–110.
36. Lambertson, D., Chen, L. & Madura, K. (2003) *Curr. Genet.* **42,** 199–208.
37. Madura, K. (2004) *Trends Biochem. Sci.* **29,** 637–640.
38. Katiyar, S., Li, G. & Lennarz, W. J. (2004) *Proc. Natl. Acad. Sci. USA* **101,** 13774–13779.
39. Schmid, S. R. & Linder, P. (1992) *Mol. Microbiol.* **6,** 283–291.
40. Rocak, S. & Linder, P. (2004) *Nat. Rev. Mol. Cell Biol.* **5,** 232–241.
41. Buelt, M. K., Glidden, B. J. & Storm, D. R. (1994) *J. Biol. Chem.* **269,** 29367–29370.
42. Tarcsa, E., Szymanska, G., Lecker, S., O'Connor, C. M. & Goldberg, A. L. (2000) *J. Biol. Chem.* **275,** 20295–20301.
43. Stone, M., Hartmann-Petersen, R., Seeger, M., Bech-Otschir, D., Wallace, M. & Gordon, C. (2004) *J. Mol. Biol.* **344,** 697–706.
44. Cai, S.-Y., Babbitt, R. W. & Marchesi, V. T. (1999) *Proc. Natl. Acad. Sci. USA* **96,** 2828–2833.
45. Laub, M., Steppuhn, J. A., Bluggel, M., Immler, D., Meyer, H. E. & Jennissen, H. P. (1998) *Eur. J. Biochem.* **255,** 422–431.
46. Sonnemann, J., Bauerle, A., Winckler, T. & Mutzel, R. (1991) *J. Biol. Chem.* **266,** 23091–23096.
47. Agell, N., Aligue, R., Alemany, V., Castro, A., Jaime, M., Pujol, M. J., Rius, E., Serratosa, J., Taules, M. & Bachs, O. (1998) *Cell Calcium* **23,** 115–121.
48. Yang, Q., O'Hanlon, D., Heizmann, C. W. & Marks, A. (1999) *Exp. Cell Res.* **246,** 501–509.
49. Deloulme, J. C., Assard, N., Mbele, G. O., Mangin, C., Kuwano, R. & Baudier, J. (2000) *J. Biol. Chem.* **275,** 35302–35310.